

iThing: Designing Next-Generation Things with Battery Health Self-Monitoring Capabilities for Sustainable IIoT

Aparna Sinha, *Student Member, IEEE*, Debanjan Das, *Senior Member, IEEE*, Venkanna Udutoalapally, *Senior Member, IEEE*, Saraju P. Mohanty, *Senior Member, IEEE*

Abstract—An accurate and reliable technique to predict rechargeable battery health proves helpful in battery-operated, low-resourced industrial IoT devices. The existing data-driven battery health prediction techniques often require a comparatively large amount of computational power for predicting the State of Health (SOH) and the Remaining Useful Life (RUL) due to most methods being feature-heavy. Further, there are very limited works for battery RUL prediction in IoT nodes. To address this issue, this paper presents a unique IoT-based sensor node framework, *iThing*, to predict the on-board battery SOH and RUL with the least computational and memory load. The *iThing* automatically extracts the voltage and time-based health indicators, which is then fed to the random learning algorithm-based methods with good learning performance for SOH and RUL prediction. The proposed Extreme Learning Machine (ELM) network provides SOH prediction with 0.0054 Root Mean Square Error (RMSE), and 0.0024 Mean Absolute Error (MAE). Random Vector Functional Link (RVFL) neural network predicted the RUL with 0.0282 RMSE and 0.021 MAE. The proposed method has been tested on three different battery datasets with varying charging policies with high accuracy. The models have been deployed successfully on an experimental hardware setup, proving its eligibility for real-time IIoT applications.

Index Terms—Industrial IoT, Battery, SOH, RUL, ELM, RVFL.

I. INTRODUCTION

IN the present time, smart nodes attached to the physical objects that are capable of sensing, processing, and communication and are connected to the internet comprise the Internet-of-Things (IoT) [1]. When the IoT is applied to industrial systems for improved reliability, security, robustness, and timeliness, it is termed the Industrial IoT, or IIoT [2]. In an IoT network, the sensor node is an important part, which has four main components - the sensor itself for data collection, the transceiver for data transfer to/from a local system or the cloud, the microcontroller for controlling both the sensor and the transceiver, and the battery for powering the entire unit.

Aparna Sinha is with the Department of Electronics & Communication Engineering, International Institute of Information Technology Naya Raipur; e-mail: aparna.sinha@ieee.org.

Debanjan Das is with the Department of Electronics & Communication Engineering, International Institute of Information Technology Naya Raipur; e-mail: debanjan@iitnr.edu.in.

Venkanna Udutoalapally is with the Department of Computer Science & Engineering, International Institute of Information Technology Naya Raipur; e-mail: venkannau@iitnr.edu.in.

Saraju P. Mohanty is with the Department of Computer Science & Engineering, University of North Texas; e-mail: saraju.mohanty@unt.edu.

The constant data collected and computed helps in various monitoring tasks in our environment.

The real-world deployment of IoT has given rise to the challenge of monitoring the health and performance of the sensor nodes themselves [3]. If one or more components of the sensor node malfunction, then the faulty data may refer to a fault in the associated system. Like any other component, the performance of the battery degrades over time. Hence, in this paper, we will focus on battery health, as the death of the battery leads to the complete failure of the sensor node. For efficient, sustainable, and uninterrupted service, a resilient IIoT-based solution has been conceptualized to communicate the battery health data, as shown in Fig. 1.

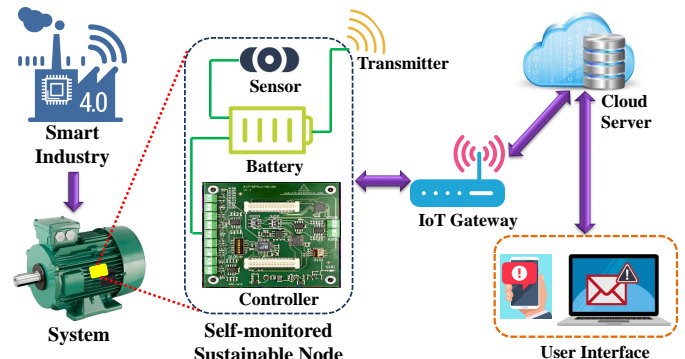


Fig. 1. A general view of the proposed resilient IIoT-based solution.

Rechargeable Lithium-ion batteries are extensively used in Electric Vehicles, Mobile Phones and Laptops, IoT devices, and many others as the power source, because they have higher energy density, lower self-discharge, and prolonged lifetime compared to other battery types [4]. Battery-powered IoT devices are mainly used to monitor the performance of various industrial systems whose uptime and functioning are critical. Recently, energy harvesters have been connected with battery systems to enhance the lifetime of the respective sensor nodes. However, Li-ion batteries degrade over time due to the formation of Solid Electrolyte Interphase film at the carbonaceous anode material [5], and the battery loses capacity and gains internal resistance. Hence, the in-built system should be able to accurately and reliably predict the State of Health (SOH) and the Remaining Useful Life (RUL) of a battery to prevent over-discharge, overcharge [6] and help in the timely replacement of the battery to avoid the failure of vital IoT

instruments. In general, the SOH measures the battery's ability to store and deliver the electrical energy. The RUL is described as the remaining cycles or time before the battery reaches its End of Life (EOL), i.e., the time needed to reach 70% or 80% of the SOH [7]. The SOH and RUL help in the short-term and long-term battery life prediction, respectively.

With rapid development in the field of Machine Learning (ML), Deep Learning (DL), and Artificial Intelligence (AI), data-driven methods have become popular as they don't require any prior internal knowledge of the system. For battery health prediction using data-driven methods, the data generation is also challenging, as Li-ion Battery has thousands of cycles, which causes reliability researchers to take several months or years before failure testing completes. Another major challenge is the extraction of suitable Health Indicators (HIs) having a high correlation with the SOH and RUL values and reduce the amount of input data in the prediction model to a large extent. Finally, a suitable model must be chosen for battery health prediction that is lightweight and easy to implement using edge-AI for real-time predictions and reduce the latency [8] [9]. To overcome these issues, a unique IoT-based framework, *iThing*, has been proposed that automatically extracts HIs from the charging cycle voltage data and predicts the battery SOH and RUL using random learning algorithms.

II. RELATED WORKS AND RESEARCH GAP

In general, there are three different methods for battery health estimation: Experimental, Model-based, and Data-driven methods. However, the experimental methods [10], and model-based methods [11] [12] are time-consuming, have very complex mathematical structures, and need vast knowledge of the complex internal battery chemistry for precise prediction. Hence, they are not suitable for online IoT applications.

Nowadays, the data-driven methods are becoming very popular, since they are non-parametric and do not depend on any prior knowledge of the internal working of the battery. For effective SOH and RUL prediction of battery, the extraction of proper HIs is important. In this regard, a NARXRNN model is used for battery SOH and RUL prediction by [13]. Similarly, a Temporal Convolutional Network (TCN) was used in a battery SOH and RUL prediction model, which is capable of capturing local regeneration of cells [14]. A transfer learning-based long short-term memory (TL-LSTM) neural network was used for battery RUL prediction for varying operating conditions [15]. A battery RUL prediction algorithm using Conditional Variational Autoencoders - Particle Filters (CVAE-PF) was proposed in [16]. All these works used raw data as input, and the model automatically extracted the HIs. Another work where the battery RUL estimation was performed successfully was by using Recurrent Neural Networks (RNN) and Genetic Algorithm (GA) [17]. However, the neural network-based methods are complex with multiple hidden layers and are difficult to implement in edge computing. The extraction of suitable HIs greatly reduces the input data for the prediction models and decreases the computational and storage load. An LSTM-based model has been used for battery health prognosis, for which complete ensemble empirical mode decomposition

TABLE I
COMPARISON OF EXISTING SOLUTIONS WITH *iThing*

Related works	HI extraction	Edge-based decisions	Computation power	Real-time prediction
Bamati <i>et al.</i> [13]	No	Yes	Low	Yes
Zhou <i>et al.</i> [14]	No	No	High	Yes
Pan <i>et al.</i> [15]	No	No	High	Yes
Jiao <i>et al.</i> [16]	No	No	High	No
Catelani <i>et al.</i> [17]	No	No	High	Yes
Cui <i>et al.</i> [18]	Yes	No	High	No
Hu <i>et al.</i> [5]	Yes	No	Medium	No
Kim <i>et al.</i> [19]	Yes	No	High	Yes
Gou <i>et al.</i> [7]	Yes	No	Medium	Yes
Greenbank <i>et al.</i> [20]	Yes	No	Medium	No
Sanz-Gorrachategui <i>et al.</i> [21]	Yes	No	Medium	Yes
Liu <i>et al.</i> [22]	Yes	No	Medium	No
Current Paper: <i>iThing</i>	Yes	Yes	Low	Yes

with adaptive noise (CEEMDAN) is used to generate the intrinsic mode functions [18]. However, this method is complex and difficult for real-time implementation in edge devices. SOH prediction using fusion-based feature selection method and GPR was implemented by Hu *et al.* [5]. Though this method was effective, the fusion-based feature selection is time-consuming and unsuitable for real-time online applications. A GPR-based method for battery health prediction by extracting the HIs from the different voltage peaks obtained during multi-stage battery charging is explained in [23], but this method is effective only for multi-stage battery charging policy. In [21], two novel HIs namely, *Capacitance peak* and *Voltage at capacitance peak* are extracted from the disturbance occurring in the low voltage part of the battery discharge cycle. But, these are noisy features and cannot be effectively extracted from the entire battery lifecycle or from different battery charging policies. A stacked LSTM was utilized for SOH prediction of battery in [19], in which the HIs were extracted from the discharge cycle of the battery. But, the discharge cycle is largely dependent on the load profiles and is not reliable for health prediction. A hybrid ensemble data-driven method can be used for SOH and RUL prediction of Li-ion batteries by Gou *et al.* [7]. This paper used the duration of equal charging voltage difference as the extracted HIs, but the voltage ranges were chosen manually. Automatic feature extraction and SOH prediction were performed using the percentile values of all the measured parameters as the ranges for HI extraction in [20]. Although this method was effective, the extraction of a large number of features made the process time-consuming and unsuitable for real-time online applications. A probabilistic Monotonic Echo State Network (MONESN)-based RUL estimation method has been proposed

by Liu *et al.* [22], where both direct HI (battery capacity) and indirect HI (time interval of equal discharging voltage difference/TIEDVD) are extracted for battery health prediction. However, the direct HI is difficult to extract and implement in real-time battery health predictions.

The comparative summary of the related works with the proposed *iThing* method is given in Table I. Although all these discussed methods have their merits, none of them are made with IoT devices in mind, since they have complex mathematical models, require high computational power, or other shortcomings mentioned previously. To overcome these shortcomings, a random learning-based method with automatic HI extraction has been proposed to predict SOH and RUL efficiently.

A. Novel Contributions of *iThing*

The major contributions of this paper are enumerated as follows:

- As of authors knowledge, this is one of the first kind of work focusing on the rechargeable battery health prediction in IoT sensor nodes using an optimised random learning algorithm-based framework, *iThing*. The random learning algorithms have a fast learning speed that aids in increasing the implementation capability.
- The presented TIECVD algorithm automatically extracts the health indicators (HIs), having high correlation with the calculated SOH and RUL, from only the battery's charging cycle.
- The ELM network is designed to predict the SOH of the three selected batteries with an average RMSE of 0.0054, which is lower compared to other existing advanced models. We affirmed the model's efficacy for RUL prediction with average RMSE value of 0.0282 for three battery sets, irrespective of their charging policies.
- The proposed *iThing* solution uses edge-as-a-service for real-time prediction of battery health. Only the predicted health data is transmitted to the cloud. This decreases the transmitter power requirement and makes it suitable to be applied in low-powered IoT devices. Further, the training dataset is reduced by more than 99%, thus reducing the storage requirement and computational complexity of the prognosis models.
- The knee-point identification from the predicted SOH of the battery enables alerting the authorities that the battery is approaching the EOL rapidly. This enhances the reliability of the remotely operated IoT sensor nodes.
- The hardware implementation proves the suitability of the *iThing* solution for on-board health prediction of battery in IoT sensor nodes.

III. PROPOSED METHODOLOGY

A. *iThing* Architecture

A unique hardware component called *iThing* has been introduced for Sustainable IoT for Battery Health Self-monitoring in Sensor Nodes. The proposed architecture for *iThing* is shown in Fig. 2. The battery is responsible for the power

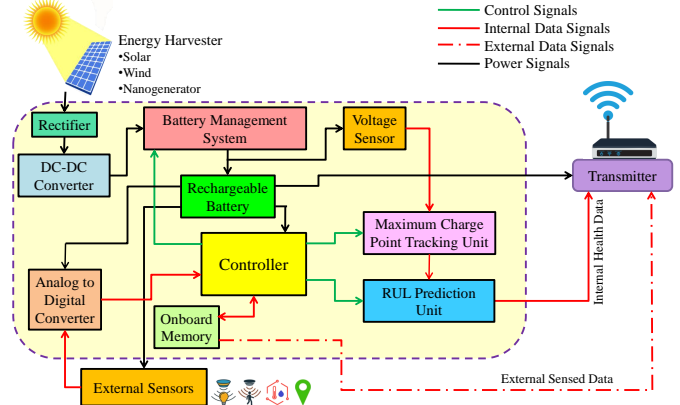


Fig. 2. Our vision of *iThing* - Battery health self-monitoring for sustainable IoT.

supply to the various components of the sensor node, like sensors, controller, and transmitter. The Battery Management System is responsible for recharging the battery in every cycle.

The voltage sensor collects the time and voltage information and sends it to the time interval of equal charging voltage difference (TIECVD) extraction unit responsible for HI extraction. The extracted HIs are then sent to the SOH and RUL Prediction Unit, where the ELM and RVFL algorithms are used to predict the SOH and RUL, respectively. Therefore, the proposed *iThing* utilizes edge-as-a-service to analyze the HIs of battery, perform edge computing and provides the necessary services for sustainable IoT applications, along with the normal sensor node functionalities. The entire calculation is done in the Sensor Node itself with minimal external interference, and the Internal Health Data is then transmitted to the cloud. This process flow is shown in Fig. 3. The external sensors responsible for measuring the environmental parameters are also collected and sent to the cloud for further processing and calculation.

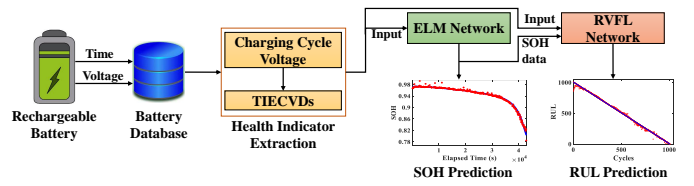


Fig. 3. Proposed process flow of *iThing* for SOH and RUL prediction of a Li-ion battery.

B. Battery Health Indicator Extraction

Typically, the reduction of capacitance and the increase of the internal resistance are the two direct HIs of a Li-ion battery. The battery SOH is the ratio of measured charge capacity (C_{curr}) to the nominal charge capacity (C_{nomi}) in Ah, as given in Eq. 1:

$$SOH = \frac{C_{curr}}{C_{nomi}} \quad (1)$$

When a battery undergoes multiple charge-discharge cycles, the maximum measured charge capacity of the battery at the

end of the charging cycle invariably decreases compared to the previous cycle as the maximum charging capacity decreases. Due to the decrease in charge capacity, the calculated SOH value also decreases proportionally. When the battery capacity decreases by 20-30%, it reaches the EOL threshold [23]. After that, the battery needs to be replaced as it becomes an unreliable power source.

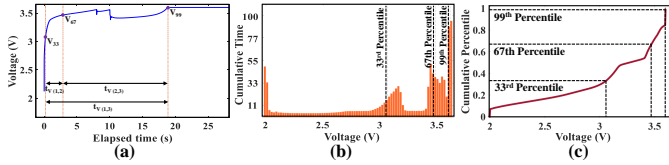


Fig. 4. (a) Voltage-time curve for one charging cycle indicating the TIECVDs, (b) Histogram, and (c) Cumulative Histogram, over the entire voltage data population.

Although the direct HIs are very effective for accurate SOH and RUL prediction of the battery, they are challenging to implement for online applications [7]. Hence, indirect HIs, such as current and voltage, are widely utilized for battery health prediction in online IoT applications. The time duration of equal terminal voltage interval during the battery's charge-discharge cycle can be considered a vital HI. However, since the discharging cycle varies with varying load profiles in highly varying online uses, the time duration of equal terminal voltage interval during the charging cycle is considered a better HI for SOH assessment. This duration gradually decreases with increasing cycle number and may be described as the time interval of an equal charging voltage difference (TIECVD), as given in Eq 2:

$$\text{TIECVD}(V_{min}, V_{max}) = t_{V_{max}} - t_{V_{min}}, \quad (2)$$

where V_{min} and V_{max} are the minimum and maximum limits of the selected charging voltage interval respectively. The time elapsed when the battery's terminal voltage becomes V_{min} and V_{max} are $t_{V_{max}}$ and $t_{V_{min}}$ respectively. Fig. 4 (a) depicts the voltage-time curve during the charging cycle indicating the extracted TIECVD features. For the entire population of voltage data given in the dataset, histogram and cumulative histogram were generated, as shown in Fig. 4 (b)-(c).

The values of V_{min} and V_{max} were determined from the cumulative histogram of the voltage values. The voltage values correlating to the 33rd, 67th and 99th percentiles were evaluated as 3.0549 V, 3.4715 V and 3.6001 V respectively. The time spent between these voltage values during the battery charging cycle is taken as the TIECVD (t_V) features, as given in Table II. The pseudo-code for the proposed HI extraction algorithm is given in Algorithm 1.

TABLE II

THE TIECVD FEATURES EXTRACTED FROM THE VOLTAGE DATA DURING THE CHARGING CYCLE OF THE BATTERY

Percentile Range	Voltage Range	Notation
33 rd to 67 th	3.0549 V to 3.4715 V	$t_{V(1,2)}$
33 rd to 99 th	3.0549 V to 3.6001 V	$t_{V(1,3)}$
67 th to 99 th	3.4715 V to 3.6001 V	$t_{V(2,3)}$

Algorithm 1 : TIECVD Extraction

Input: 1. $V(v_1, v_2, \dots, v_p)$ {Charging Voltage data}
Input: 2. $t(t_1, t_2, \dots, t_p)$ {Time data in charging cycle}
1: Calculate 33rd, 67th and 99th percentiles of V as v_{p-33} , v_{p-67} and v_{p-99} respectively
2: **for** $i = 1$ to p **do**
3: **if** $V(i) > v_{p-33}$ **then**
4: $t_{p-33} = t(i)$
5: **break**
6: **end if**
7: **end for**
8: **for** $j = i$ to p **do**
9: **if** $V(j) > v_{p-67}$ **then**
10: $t_{p-67} = t(j)$
11: **break**
12: **end if**
13: **end for**
14: **for** $k = j$ to p **do**
15: **if** $V(k) > v_{p-99}$ **then**
16: $t_{p-99} = t(k)$
17: **break**
18: **end if**
19: **end for**
20: $t_{V(1,2)} = t_{p-67} - t_{p-33}$
21: $t_{V(1,3)} = t_{p-99} - t_{p-33}$
22: $t_{V(2,3)} = t_{p-99} - t_{p-67}$
Output: $t_{V(1,2)}, t_{V(1,3)}, t_{V(2,3)}$ {Extracted TIECVDs}

C. Battery SOH Prediction

The extracted HIs of the Li-ion battery are used for the SOH prediction. For this purpose, the Extreme Learning Machine (ELM) is used. It is an effective and lightweight training algorithm for single hidden layer feed-forward neural networks (SLFNs). Since the ELM does not employ a back-propagation algorithm, the weights between the input and hidden layer are assigned randomly; only the weights between the hidden and output layer are learned analytically [24]. The algorithm has a faster learning speed as it avoids iterations. Further, the presence of random hidden nodes leads to good generalization capability. The structure of the ELM model used for battery SOH prediction in this paper is given in Fig. 5 (a).

Let us consider that the weight between input and hidden layer is represented by ω , while b stands for the bias of the hidden layer and β denotes the output weight. A training set is given as $S = (\mathbf{a}_i, r_i)|\mathbf{a}_i = (a_{i1}, \dots, a_{in})^T \epsilon R^n, r_i = (r_{i1}, \dots, r_{in})^T \epsilon R^m$, where \mathbf{a}_i and r_i represent the input value and target respectively. Then, the output \mathbf{z} of ELM model having \hat{N} hidden neurons can be given by:

$$\sum_{k=1}^{\hat{N}} \beta_k g_E(\omega_k \mathbf{a}_j + b_k) = \mathbf{z}_j, j = 1, 2, \dots, N, \quad (3)$$

where $g_E(x)$ denotes the activation function of the hidden layer. Here *relu* has been taken as the activation function of

the ELM model used for battery SOH prediction. The formula given in Eq. 3 can be abbreviated as:

$$\mathbf{H}\beta = \mathbf{T}, \quad (4)$$

where \mathbf{H} and \mathbf{T} represent the hidden layer output matrix and the target matrix respectively. Therefore, from Eq. 4, the output weights can be evaluated as:

$$\beta = \mathbf{H}^\dagger \mathbf{T}, \quad (5)$$

where \mathbf{H}^\dagger denotes the Moore–Penrose generalized inverse of the matrix \mathbf{H} . Hence, the primary aim of the ELM training is not only to find the minimum training error but also to determine the least norm of the output weights. It has been quantitatively proved that the learning speed of ELM is a thousand times faster and has much less computational burden compared to the traditional models [7]. This has motivated the authors to use the ELM network for SOH prediction of the Li-ion batteries in the current paper. A keras-like numpy implementation of ELM has been performed in this paper using the python libraries such as Numpy and Tensorflow [25]. The ELM model used in this paper for battery SOH prediction employs 100 hidden nodes and *ReLU* activation function, and the cost function (*C*) is taken as 1 (default value). The three extracted HIs, $t_{V(1,2)}$, $t_{V(1,3)}$ and $t_{V(2,3)}$, are taken as inputs to the ELM network.

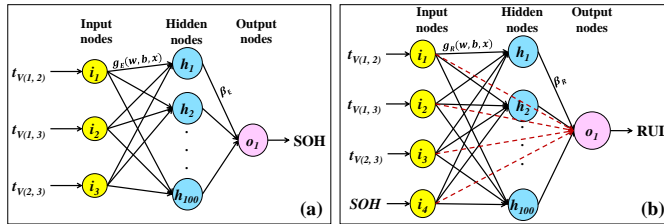


Fig. 5. The structures of (a) ELM and (b) RVFL used for battery SOH and RUL prediction, respectively.

D. Battery RUL Prediction

The extracted HIs and the SOH predicted from the ELM network are used for the RUL prediction of the Li-ion battery. The Random Vector Functional Link (RVFL) neural network was employed for this purpose. The RVFL is also a type of SLFN where the input and output layers are connected directly. This is the significant difference between the ELM and RVFL networks. Fig. 5 (b) illustrates the structure of the RVFL-based RUL prediction model.

Let us consider the input data $\mathbf{X} = [x_1, x_2, \dots, x_n]$ is mapped to the hidden layer using the non-linear activation function $g_R(w_j^T \mathbf{X} + b_j)$, where w_j and b_j are the weight and bias of the j^{th} hidden node respectively. For N input nodes and J hidden nodes, the RVFL network is represented by [7]:

$$f(\mathbf{X}) = \sum_{j=1}^J \beta_j g_R(w_j^T \mathbf{X} + b_j) + \sum_{j=J+1}^{J+N} \beta_j x_j, \quad (6)$$

where β_j represents the j^{th} weight terms. The least-squares method-based optimization of hidden and output layer weights

reduces the output error of the trained RVFL model, using the equation:

$$\min \epsilon^2 = \frac{1}{2P} \sum_{p=1}^P (t^{(p)} - B^t d^{(p)})^2, \quad (7)$$

where P is the number of training samples with index (p) , B^t contains $(J + N)$ weight values and d represents the output nodes vector. Random sampling from the uniform distribution [-1, 1] gives the weights between the input and hidden layers in RVFL. The RVFL network reportedly shows much less computation time than the traditional methods, which persuaded the authors to use it for RUL prediction. In this paper, the RVFL network uses 100 hidden nodes and *ReLU* activation function for accurate RUL prediction. Apart from the three extracted TIECVD features, the SOH obtained as output from the ELM network is also given as input to the RVFL network. A deep RVFL network using python was used in this paper for RUL prognosis [26].

IV. CASE STUDY

A. Dataset description

This section will discuss the dataset used for the battery aging test. The dataset is drawn from experiments performed by Severson *et al.* [27], which uses Lithium Iron Phosphate (LFP) cells fabricated by A123 Systems (APR18650M1A). The nominal capacity and the nominal voltage are 1.1 Ah and 3.3 V, respectively.

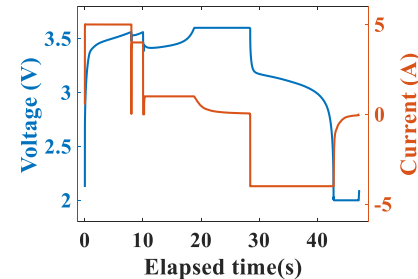


Fig. 6. Current versus time and voltage versus time graph for one charge-discharge cycle for the dataset used.

The cells have been charged under a two-step fast charging condition. The battery is initially charged in Constant Current (CC) mode at 5 Coulomb until the cell reaches 67% SoC. After that, it is charged in CC mode at 4 Coulomb until the cell reaches 80% SoC. Charging time is fixed at 10 minutes for 0% to 80% SoC. Then, the battery is charged at 1 Coulomb Constant Current–Constant Voltage (CC–CV) mode. As per the manufacturer's specifications, the lower and upper cut-off potentials are 2 V and 3.6 V, respectively. The battery is discharged at 4 Coulomb CC mode. The current and voltage graphs for one charge-discharge cycle are shown in Fig. 6.

Three batteries with different charging policies and life cycles are chosen from *Batch - 2018-04-12*. The specifications of the selected batteries along with their charging policies are shown in Table III. The training, testing and validation data are taken as 70%, 15% and 15% of the entire dataset, respectively.

TABLE III
DESCRIPTION OF THE BATTERIES SELECTED FROM THE DATASET

Battery ID	Charging policy	Channel ID	Life cycle
el150800737329	5C(67%)-4C-newstructure	10	1008
el150800737270	5.3C(54%)-4C-newstructure	18	1039
el150800737325	5.6C(36%)-4.3C-newstructure	28	1155

V. RESULT AND DISCUSSION

A. Evaluation of the HIs

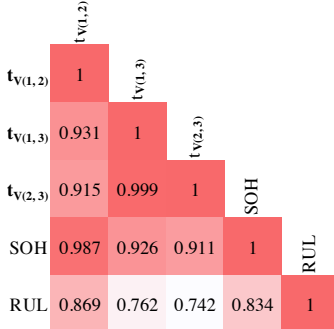


Fig. 7. Correlation Matrix showing the dependencies of the extracted HIs with the SOH and RUL.

The TIECVD features extracted from the voltage and time values of the battery charging cycle are used to predict the battery's SOH and RUL. Before applying these features in the ELM and RVFL models, it is vital to analyze the dependency of SOH and RUL on the extracted HIs. There are different correlation analysis methods, out of which only Pearson's correlation [28] coefficient accepts non-ordinal data. But Pearson's coefficient calculation assumes that its data is linear, which is not the case in this paper. Hence, the data is divided, and a piece-wise analysis is performed.

Let us assume x_i is the i^{th} feature of the feature set with size n, and y_i is the i^{th} target of the target set with size n. Hence, the Pearson's correlation coefficient is calculated using the following formula [28]:

$$r = \frac{\sum_{i=1}^n (x_i - \bar{x})(y_i - \bar{y})}{\sqrt{\sum_{i=1}^n (x_i - \bar{x})^2} \sqrt{\sum_{i=1}^n (y_i - \bar{y})^2}}, \quad (8)$$

where \bar{x} is

$$\bar{x} = \frac{1}{n} \sum_{i=1}^n x_i \quad (9)$$

and \bar{y} is

$$\bar{y} = \frac{1}{n} \sum_{i=1}^n y_i \quad (10)$$

Fig. 7 depicts the correlation of the extracted HIs with actual SOH and RUL. It is understood that the extracted TIECVD features have a high correlation with SOH and RUL, and hence they can be used for accurate prediction of battery health.

B. SOH Prediction Results

The proposed ELM-based battery health prediction framework is used to predict the SOH of three different batteries. This paper evaluates the prediction results based on Root Mean

Square Error (RMSE) and Mean Absolute Error (MAE) values using the Eq. 11-12:

$$RMSE = \sqrt{\frac{\sum_{i=1}^n (RUL_{actual,i} - RUL_{predicted,i})^2}{n}}, \quad (11)$$

$$MAE = \frac{|RUL_{actual} - RUL_{predicted}|}{n}. \quad (12)$$

Lower values of RMSE and MAE indicate higher accuracy of prediction. The SOH prediction results of three different batteries are summarized in Table IV. The low runtime in each case indicates the feasibility of real-time SOH prediction using the proposed model.

TABLE IV
SOH PREDICTION RESULTS FOR THREE DIFFERENT BATTERIES

Battery ID	Test RMSE (%)	Valid. RMSE (%)	Test MAE (%)	Valid. MAE (%)	Runtime (s)
el150800737329	0.0024	0.0063	0.0012	0.0017	0.078
el150800737270	0.0081	0.0062	0.0024	0.0044	0.0935
el150800737275	0.0053	0.0037	0.003	0.0012	0.0937

The proposed method is executed at different starting prediction points to verify its effectiveness. Fig. 8(a)-(c) demonstrates the SOH prediction results for the three chosen batteries, respectively, when the prediction starting points are set to 60%, 70%, and 80% of the battery lifetime. The RMSE and MAE values for all these predictions are represented in bar graph form, as shown in Fig. 8(d). These results show that the proposed method can effectively predict the SOH during the entire battery life, and the accuracy increases if the prediction starts at a later point.

C. Battery RUL Prediction

Similar to the SOH prediction model, the performance of the RUL prediction model using the RVFL network has been evaluated using MSE, RMSE, and MAE. Table V shows the RUL prediction results for the three chosen batteries. The low error values prove that the proposed model can accurately predict the battery RUL so that the battery can be changed timely without any loss of monitoring data. Fig. 9 (a)-(c) demonstrates the closeness of the actual RUL with the predicted RUL for all three batteries. The training and validation loss curves of three batteries for different epochs are given in Fig. 9 (d)-(f).

TABLE V
RUL PREDICTION RESULTS FOR THREE DIFFERENT BATTERIES

Battery ID	MSE(%)	RMSE(%)	MAE(%)	95% CI
el150800737329	0.0006	0.0247	0.0163	[486, 522]
el150800737270	0.0014	0.0384	0.0304	[502, 539]
el150800737275	0.004	0.0216	0.0163	[558, 597]

For better understanding of the error committed by the proposed method, the Absolute Error (AE) gives a quick and more effective information about the proposed model. The RVFL network is trained using 80% of the samples and the AE for the three batteries are given in Table VI.

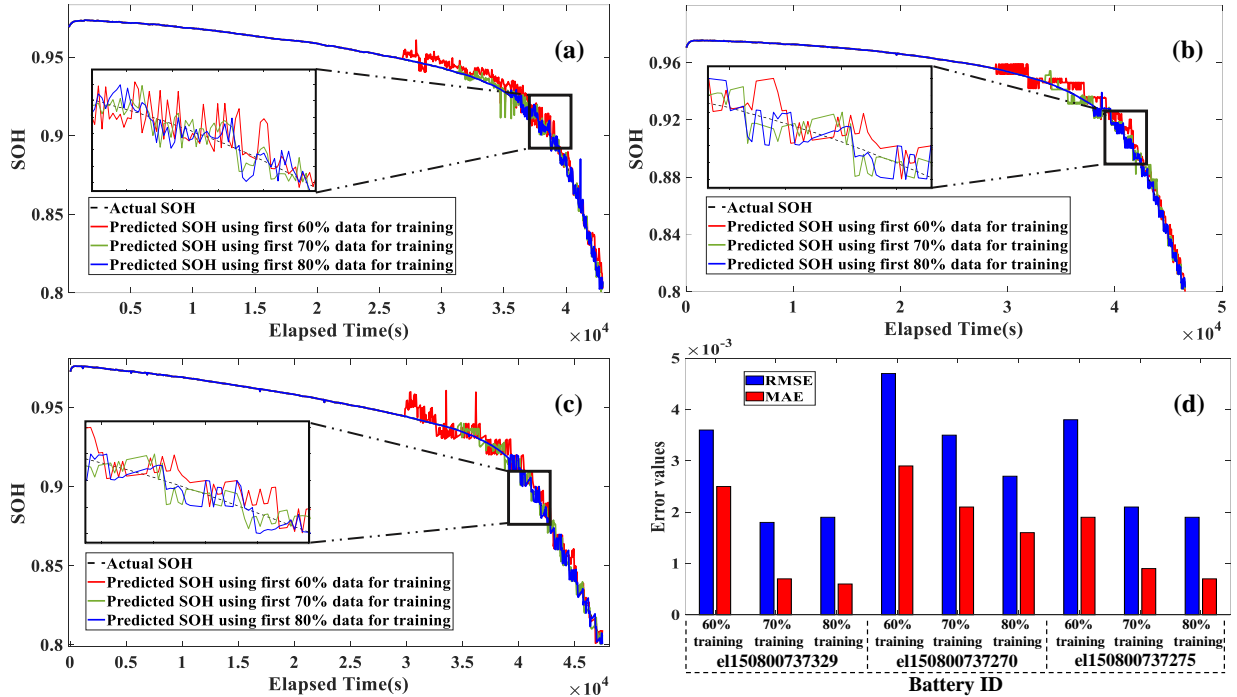


Fig. 8. Predicted SOH graph with different starting prediction points for batteries (a) el150800737329, (b) el150800737270 and (c) el150800737275; (d) Error values for the SOH predictions.

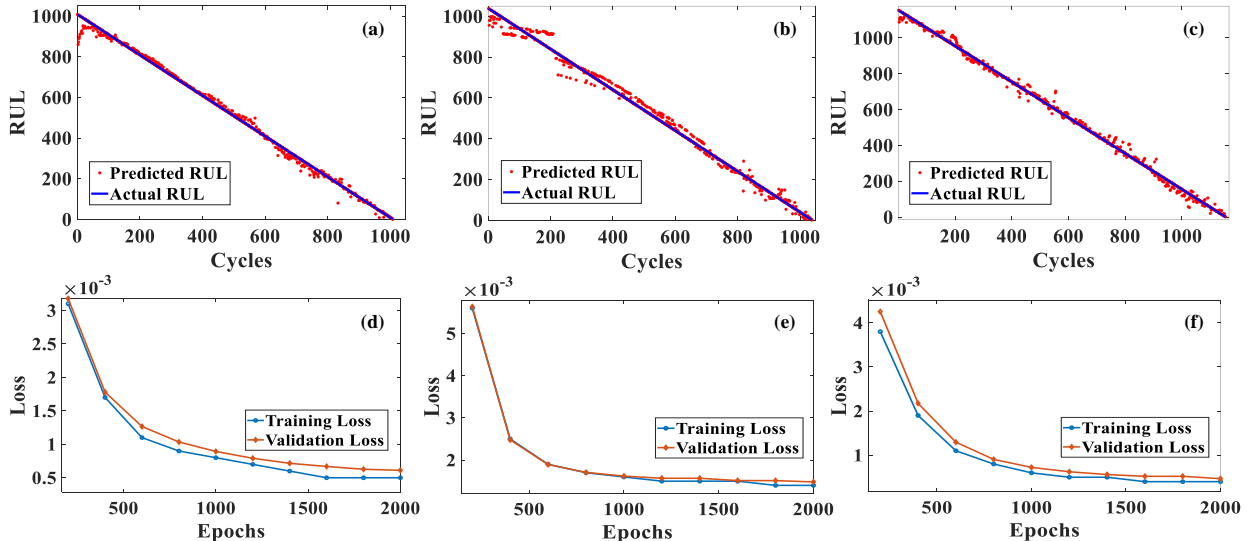


Fig. 9. Closeness of the actual RUL with the predicted RUL for batteries (a) el150800737329, (b) el150800737270 and (c) el150800737275; Training and Validation loss curves for batteries (d) el150800737329, (e) el150800737270 and (f) el150800737275.

TABLE VI
ABSOLUTE ERROR FOR RUL PREDICTION OF THREE DIFFERENT BATTERIES

Battery ID	Actual RUL	Predicted RUL	AE
el150800737329	806 cycles	815 cycles	9 cycles
el150800737270	831 cycles	824 cycles	7 cycles
el150800737275	923 cycles	912 cycles	11 cycle

D. Identification of Knee Point

The capacity fade of a Li-ion battery over time leads to reduced SOH value. The point after which the value of SOH

degrades rapidly is termed as the *knee-point* of the SOH curve. Identifying knee-point is essential as the battery swiftly approaches its EOL and becomes unfit to be used reliably. In this work, the early and late life SOH curve gradients are evaluated using Linear regression. The point where the gradient intersection point perpendicularly meets the SOH curve is considered to be the knee-point, as shown in Fig. 10. For battery el150800737329, the knee-point occurs when battery SOH is 0.92.

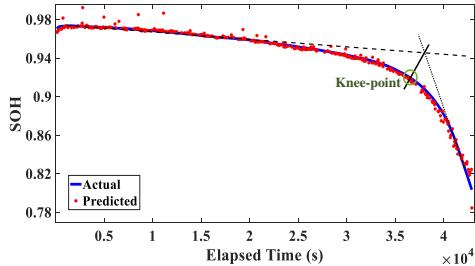
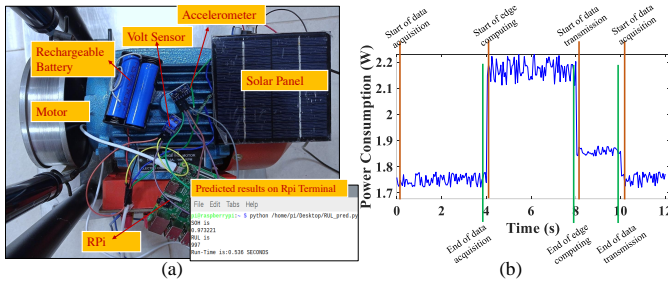


Fig. 10. Calculation of the knee point in battery SOH graph.

Fig. 11. (a) *iThing* hardware setup, (b) Power consumption during battery health data acquisition, edge computing and transmission.

E. Experimental setup and deployment

The experimental hardware setup of the *iThing* is shown in Fig. 11(a). A sensor node is designed for monitoring the health of a motor based on the vibration data. The rechargeable Li-ion batteries with 3.7 V nominal voltage and 2.2 Ah nominal capacity are used in this hardware system. The other components used in the hardware setup are listed in Table VII. The *iThing* was successfully implemented in the designed sensor node, and edge computation was performed on the Raspberry pi within a second. The practical implementation result is shown in Fig. 11(b). The battery SOH and RUL are predicted as 0.973 and 997 cycles, respectively. Thus, the proposed technique can be deployed on-board for real-time SOH and RUL prediction of a rechargeable battery.

TABLE VII
COMPONENT SPECIFICATIONS USED IN THE HARDWARE SETUP

Component name	Part number
Micro-controller	Raspberry Pi 3B
Battery Management System	1S 18650
DC-DC converter	LM2596
Voltage sensor	BE-000975
Accelerometer	MPU6050
Battery	INR18650
Energy harvester	Solar panel (12V, 1.8W)

F. Computational efficiency

Since extracting TIECVD features reduces the training data by a lot, only 0.4% of the data was used in training the model. Hence, the HIs extracted and stored for training the SOH and RUL prediction models come down to only 39 KB of data, which can be discarded after the model's training if necessary, saving even more space. Using an off-the-shelf

computing device with a RAM capacity of 1GB, the model can be deployed for real-time RUL prediction of battery. To determine the power consumed by the computing device for data acquisition, edge computing and data transmission, its current and voltage values were measured using the National Instruments' myDAQ module. This provides the power consumption profile for the different working modes, as shown in Fig. 11(b). It is to be noted that this power profile is only based on the health prediction of on-board batteries. Moreover, the edge computing occurs only at scheduled intervals and thus the power consumption is limited.

G. Comparison with the State-of-the-Art Models

For further performance evaluation of the proposed method, the testing RMSE and MAE values of the ELM and RVFL algorithms have been compared with various State-of-the-Art (SOTA) models that are lightweight and edge-deployable. The SOTA models considered in this paper are Random Forest/RF (Ensemble algorithm), Support Vector Regression/SVR (Machine Learning), and Echo State Network/ESN (Random Learning). Table VIII shows the comparison of SOH prediction performance using different SOTA algorithms. The ELM model gave the least RMSE compared to the other models. Similarly, Table IX compares the performance of several RUL prediction models, among which the RVFL network gave the lowest RMSE.

TABLE VIII
SOH PREDICTION PERFORMANCE USING DIFFERENT ALGORITHMS

Algorithm used	Test RMSE (%)	Test MAE (%)	Valid RMSE (%)	Valid MAE (%)
ELM	0.0024	0.0012	0.0063	0.0017
RVFL	0.0558	0.0528	0.0569	0.0530
ESN	0.0058	0.0038	0.0081	0.0043
RF	0.0034	0.0024	0.0036	0.0024
SVR	0.0658	0.062	0.0667	0.063

TABLE IX
RUL PREDICTION PERFORMANCE USING DIFFERENT ALGORITHMS

Algorithm used	Testing RMSE (%)	Testing MAE (%)	Valid RMSE (%)	Valid MAE (%)
RVFL	0.0247	0.0163	0.0233	0.0158
ELM	0.0545	0.0388	0.0536	0.0374
ESN	0.4409	0.3403	0.4365	0.3396
RF	0.0296	0.0105	0.0291	0.01
SVR	0.0892	0.0647	0.089	0.0643

VI. CONCLUSION AND FUTURE SCOPE

There can be significant loss of vital monitoring information due to the failure of the IoT sensor node caused by the death of the battery. It is a challenging task to predict the battery SOH and RUL accurately and efficiently using less computational and storage capability, suitable for the low-powered and remotely operated IoT devices. Considering these problems, a unique *iThing* architecture with Battery health self-monitoring capability has been proposed for uninterrupted power supply to the IoT sensor nodes in smart industries.

The main conclusions of the current paper are listed as follows: (1) An automated HI extraction technique based on the charging cycle voltage has been proposed that has a high correlation with SOH and RUL parameters. (2) ELM-based model has been used for SOH prediction of the battery that gives only 0.0024% RMSE and 0.0012% MAE. (3) The RUL prediction of the battery is performed accurately by the RVFL network with 0.0247% RMSE and 0.0163% MAE. (d) The data from three different battery cells have been tested to prove the suitability of the proposed method for SOH and RUL prediction. Thus, we confirm that the model is accurate and efficient enough to be implemented in IoT devices and can benefit the user by alerting them to timely and planned replacement of the battery cell to avoid any crucial failures. Although this paper provides a novel method for battery health estimation, there are still some areas for improvement for this model. For example, the temperature of the battery, which is a critical parameter, was not considered. This can be taken into account for further work on the *iThing* technique. Only one type of battery (*LiFePO₄*) was experimented with and used to train and test the proposed method, which can be considered for future work. Further, the effectiveness and reliability of the proposed *iThing* for SOH and RUL prediction can be checked practically after months of running the battery. Moreover, the health prediction of a battery in its second life can also be a viable option for our future work.

REFERENCES

- [1] S. K. Ram, S. R. Sahoo, B. B. Das, K. Mahapatra, and S. Mohanty, "Eternal-Thing: A Secure Aging-Aware Solar-Energy Harvester Thing for Sustainable IoT," *IEEE Trans. Sustain. Comput.*, pp. 1–1, 2020. [Online]. Available: <https://doi.org/10.1109/TSUSC.2020.2987616>
- [2] D. Yang, A. Mahmood, S. A. Hassan, and M. Gidlund, "Guest Editorial: Industrial IoT and Sensor Networks in 5G-and-Beyond Wireless Communication," *IEEE Trans. Ind. Informat.*, vol. 18, no. 6, pp. 4118–4121, 2022.
- [3] R. Zhang, D. Yuan, and Y. Wang, "A Health Monitoring System for Wireless Sensor Networks," in *2007 2nd IEEE Conference on Industrial Electronics and Applications*. IEEE, 2007, pp. 1648–1652.
- [4] K. Liu, Q. Peng, H. Sun, M. Fei, H. Ma, and T. Hu, "A Transferred Recurrent Neural Network for Battery Calendar Health Prognostics of Energy-Transportation Systems," *IEEE Trans. Ind. Informat.*, pp. 1–1, 2022.
- [5] X. Hu, Y. Che, X. Lin, and S. Onori, "Battery Health Prediction Using Fusion-Based Feature Selection and Machine Learning," *IEEE Trans. Transport. Electricif.*, vol. 7, no. 2, pp. 382–398, 2020.
- [6] S. K. Mandal, R. N. Mahapatra, P. S. Bhojwani, and S. P. Mohanty, "IntellBatt: Toward a Smarter Battery," *Computer*, vol. 43, no. 3, pp. 67–71, 2010.
- [7] B. Gou, Y. Xu, and X. Feng, "State-of-Health Estimation and Remaining-Useful-Life Prediction for Lithium-Ion Battery Using a Hybrid Data-Driven Method," *IEEE Trans. Veh. Technol.*, vol. 69, no. 10, pp. 10 854–10 867, 2020.
- [8] V. K. Rathi, N. K. Rajput, S. Mishra, B. A. Grover, P. Tiwari, A. K. Jaiswal, and M. S. Hossain, "An edge AI-enabled IoT healthcare monitoring system for smart cities," *Computers & Electrical Engineering*, vol. 96, p. 107524, 2021.
- [9] A. H. Sodhro, S. Pirbhulal, and V. H. C. De Albuquerque, "Artificial intelligence-driven mechanism for edge computing-based industrial applications," *IEEE Transactions on Industrial Informatics*, vol. 15, no. 7, pp. 4235–4243, 2019.
- [10] C. Lyu, T. Zhang, W. Luo, G. Wei, B. Ma, and L. Wang, "SOH Estimation of Lithium-ion Batteries Based on Fast Time Domain Impedance Spectroscopy," 06 2019, pp. 2142–2147.
- [11] P. A. Topan, M. N. Ramadan, G. Fathoni, A. I. Cahyadi, and O. Wahyunggoro, "State of Charge (SOC) and State of Health (SOH) Estimation on Lithium Polymer Battery via Kalman Filter," in *2016 2nd International Conference on Science and Technology-Computer (ICST)*, 2016, pp. 93–96.
- [12] J. He, Z. Wei, X. Bian, and F. Yan, "State-of-Health Estimation of Lithium-Ion Batteries Using Incremental Capacity Analysis Based on Voltage–Capacity Model," *IEEE Trans. Transport. Electricif.*, vol. 6, no. 2, pp. 417–426, 2020.
- [13] S. Bamati and H. Chaoui, "Lithium-ion Batteries Long Horizon Health Prognostic Using Machine Learning," *IEEE Trans. Energy Convers.*, 2021.
- [14] D. Zhou, Z. Li, J. Zhu, H. Zhang, and L. Hou, "State of Health Monitoring and Remaining Useful Life Prediction of Lithium-ion Batteries Based on Temporal Convolutional Network," *IEEE Access*, vol. 8, pp. 53 307–53 320, 2020.
- [15] D. Pan, H. Li, and S. Wang, "Transfer Learning-Based Hybrid Remaining Useful Life Prediction for Lithium-Ion Batteries Under Different Stresses," *IEEE Trans. Instrum. Meas.*, vol. 71, pp. 1–10, 2022.
- [16] R. Jiao, K. Peng, and J. Dong, "Remaining useful life prediction of lithium-ion batteries based on conditional variational autoencoders-particle filter," *IEEE Trans. Instrum. Meas.*, vol. 69, no. 11, pp. 8831–8843, 2020.
- [17] M. Catelani, L. Ciani, R. Fantacci, G. Patrizi, and B. Picano, "Remaining useful life estimation for prognostics of lithium-ion batteries based on recurrent neural network," *IEEE Trans. Instrum. Meas.*, vol. 70, pp. 1–11, 2021.
- [18] Y. Cui and Y. Chen, "Prognostics of Lithium-ion Batteries Based on Capacity Regeneration Analysis and Long Short-term Memory Network," *IEEE Trans. Instrum. Meas.*, pp. 1–1, 2022.
- [19] A. Kim and S. Lee, "Online State of Health Estimation of Batteries under Varying Discharging Current Based on a Long Short Term Memory," in *2021 15th International Conference on Ubiquitous Information Management and Communication (IMCOM)*. IEEE, 2021, pp. 1–6.
- [20] S. Greenbank and D. Howey, "Automated Feature Extraction and Selection for Data-Driven Models of Rapid Battery Capacity Fade and End of Life," *IEEE Trans. Ind. Informat.*, 2021.
- [21] I. Sanz-Gorrachategui, P. Pastor-Flores, M. Pajovic, Y. Wang, P. V. Orlik, C. Bernal-Ruiz, A. Bono-Nuez, and J. S. Artal-Sevil, "Remaining useful life estimation for LFP cells in second-life applications," *IEEE Trans. Instrum. Meas.*, vol. 70, pp. 1–10, 2021.
- [22] D. Liu, W. Xie, H. Liao, and Y. Peng, "An integrated probabilistic approach to lithium-ion battery remaining useful life estimation," *IEEE Trans. Instrum. Meas.*, vol. 64, no. 3, pp. 660–670, 2014.
- [23] X. Hu, Y. Che, X. Lin, and Z. Deng, "Health prognosis for electric vehicle battery packs: A data-driven approach," *IEEE/ASME Trans. Mechatronics*, vol. 25, no. 6, pp. 2622–2632, 2020.
- [24] J. Wang, S. Lu, S.-H. Wang, and Y.-D. Zhang, "A Review on Extreme Learning Machine," *Multimedia Tools and Applications*, pp. 1–50, 2021.
- [25] "Numpy-ELM," <https://github.com/otenim/Numpy-ELM>, accessed: 2022-06-21.
- [26] "Deep-RVFL," <https://github.com/Xuyang-Huang/Ensemble-Deep-RVFL-python>, accessed: 2022-06-21.
- [27] K. A. Severson *et al.*, "Data-Driven Prediction of Battery Cycle Life before Capacity Degradation," *Nature Energy*, vol. 4, no. 5, pp. 383–391, May 2019.
- [28] M. Franzese and A. Iuliano, "Correlation Analysis," in *Encyclopedia of Bioinformatics and Computational Biology*, S. Ranganathan, M. Gribkoff, K. Nakai, and C. Schönbach, Eds. Oxford: Academic Press, 2019, pp. 706–721.



Aparna Sinha (Student Member, IEEE) received the B.Tech. degree in Electronics and Communication Engineering from Techno India Saltlake, Kolkata, in 2013, and the M.Tech. degree in VLSI Design from Department of Radiophysics and Electronics, University of Calcutta, in 2020. She is currently working towards the Ph.D. degree from IIIT Naya Raipur, India. Her current research interest includes IoT and Sensors.



Debanjan Das (Senior Member, IEEE) received the B.Tech. degree in applied Electronics and Instrumentation engineering from the Heritage Institute of Technology, Kolkata, in 2009, the M.Tech. degree in Instrumentation from Indian Institute of Technology, Kharagpur, in 2011, and the Ph.D. degree in Electrical Engineering from Indian Institute of Technology, Kharagpur, in 2016. He is an Assistant Professor with Dr. SPM IIIT Naya Raipur. His current research interests include IoT-Smart Sensing, Signal Processing, Bioimpedance, Instrumentation.

He has been a member of the IEEE Engineering in Medicine and Biology Society, Measurement and Instrumentation Society.



Venkanna Udutoorapally (Senior Member, IEEE) obtained his Ph.D. degree from the National Institute of Technology, Tiruchirappalli (NITT), in 2015. Since 2005, he has been in the teaching profession and currently he is an Assistant Professor in the Department of CSE, IIIT Naya Raipur (IIIT- NR). He has eight years of teaching experience and seven years of research experience. His research interests include IoT, Software Defined Networks, Network Security, Wireless Ad hoc, and Sensor network. He is a recipient of best paper award in IEEE-ANTS-

2019 conference.



Saraju P. Mohanty (SM'08) received the bachelor's degree (Honors) in Electrical Engineering from the Orissa University of Agriculture and Technology, Bhubaneswar, in 1995, the master's degree in Systems Science and Automation from the Indian Institute of Science, Bengaluru, in 1999, and the Ph.D. degree in Computer Science and Engineering from the University of South Florida, Tampa, in 2003. He is a Professor with the University of North Texas. His research is in Smart Electronic Systems which has been funded by National Science Foundations

(NSF), Semiconductor Research Corporation (SRC), U.S. Air Force, IUSSTF, and Mission Innovation. He has authored 450 research articles, 5 books, and invented 4 granted and 4 pending patents. His Google Scholar h-index is 47 and i10-index is 200 with 10,000 citations. He is a recipient of 14 best paper awards, Fulbright Specialist Award in 2020, IEEE Consumer Electronics Society Outstanding Service Award in 2020, the IEEE-CS-TCVLSI Distinguished Leadership Award in 2018, and the PROSE Award for Best Textbook in Physical Sciences and Mathematics category in 2016. He has delivered 15 keynotes and served on 13 panels at various International Conferences. He is ranked among top 2% faculty in the world with 30th rank for year 2019 and 25th rank for year 2020 in the "Computer Hardware & Architecture" area.